

Electrochemical “Switching” of Si(100) Modular Assemblies

Simone Ciampi,[†] Michael James,^{†,‡} Guillaume Le Saux,[†] Katharina Gaus,[§] and J. Justin Gooding^{*,†}

[†]School of Chemistry, The University of New South Wales, Sydney, NSW 2052, Australia

[‡]Bragg Institute, Australian Nuclear Science and Technology Organisation (ANSTO), Locked Bag 2001, Kirrawee DC, NSW 2232, Australia

[§]Centre for Vascular Research, The University of New South Wales, Sydney, NSW 2052, Australia

S Supporting Information

ABSTRACT: We report on a modular approach for producing well-defined and electrochemically switchable surfaces on Si(100). The switching of these surfaces is shown to change a Si(100) surface from resistant to cell adsorption to promoting cell adhesion. The electrochemical conversion of the modified electrode surface is demonstrated by X-ray photoelectron spectroscopy, X-ray reflectometry, contact angle and cell adhesion studies.

The dynamic behavior of living mammalian cells is not only regulated by the cell itself but also influenced by a variety of external stimuli, including cell–substrate interactions.¹ The ability of cells to sense characteristics of the surface to which they adhere is an active area of research encompassing cell biology and surface chemistry, an area known as mechanobiology or mechanosensing.² Biomimetic adhesive substrates³ with tailored physical-chemical features are now used as a tool to elucidate mechanistic information on eukaryotic cell processes such as signal transduction, adhesion, and migration.⁴ Variation in surface features, such as the density and distribution of cell adhesion ligands, rapidly translates to cells adjusting their shape and motility.² A number of chemically well-defined biomimetic substrates have been designed to clarify the relationship between spatial distribution of cell-adhesive ligands and activation of the cell’s sensing and signaling machinery.⁵ To advance further our understanding of the dynamics of cellular processes requires dynamic control over the interface properties of biomimetic surfaces.^{4,6} Because of the noninvasive and quantitative nature of redox reactions, electrochemically programmable films hold considerable promise as dynamic substrates.^{6a,7} To date, gold has undoubtedly been the metal of choice for generating these model substrates.⁸ However, because of both the vast resources of organometallic chemistry⁹ and its role as workhorse in the microelectronic industry,¹⁰ silicon has attracted growing interest¹¹ as substrate material for the production of high-quality and highly stable monolayers¹² on a substrate that does not quench fluorescence to the extent of gold.¹³

In this work, we merged an approach for producing well-defined surface chemistry that prevents cell adhesion with the ability to electrochemically switch the chemistry to allow mammalian cells to adhere. This enabled the creation of model surfaces that can be dynamically modulated where the interaction between cell and material is defined at the molecular

level. As depicted in Figure 1, high-quality monolayers were formed on nonoxidized silicon surfaces via hydrosilylation of

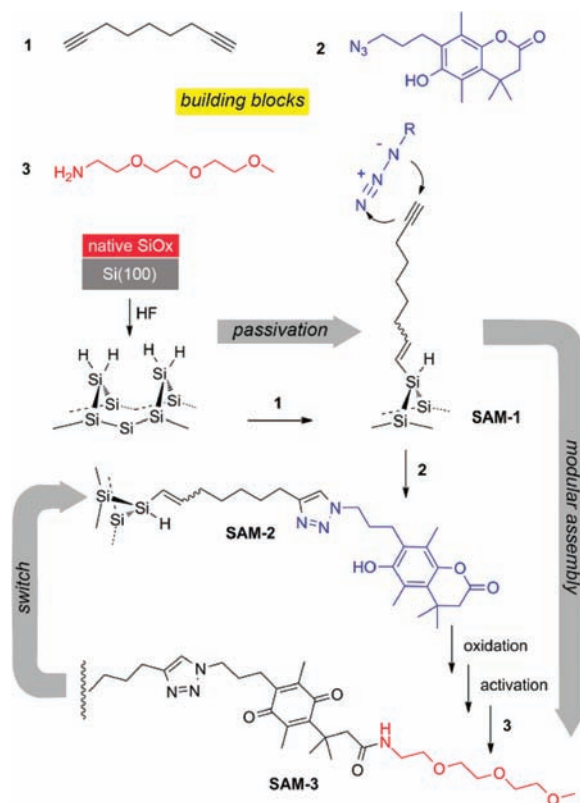


Figure 1. “Switchable” modular assemblies. Attachment and functionalization of redox-sensitive linker 2 on a Si(100) electrode.

1,8-nonadiyne (**1**) (to ensure silicon passivation and operation in aqueous environments¹⁴). To this monolayer, the azide-tagged coumarin molecule **2** was attached via the Huisgen 1,5-dipolar cycloaddition reaction, the archetypal “click” reaction (SAM-1 to SAM-2; Figure 1). The quinone moiety on SAM-3 can be electrochemically converted back to SAM-2 via what is known as the “trimethyl lock” lactonization system.¹⁵ The trimethyl lock scheme¹⁶ [Scheme S1 in the Supporting Information (SI)] was developed in the 1970s to facilitate

Received: October 25, 2011

Published: December 16, 2011

cyclization reactions¹⁷ and revisited more recently in the preparation of redox-sensitive resins for solid-phase peptide synthesis¹⁸ and in the release of short peptides involved in the adhesion of cells on gold substrates.^{7a} The conversion of SAM-3 back to the precursor SAM-2 means a new SAM-3 could be prepared, and hence, the system can be chemically switched in one direction and electrochemically switched back in the opposite direction. In our case, oligo(ethylene oxide) (OEO) 3, as a cell-adhesion-resistant molecule, was attached to SAM-2 to create a surface to which cells do not adhere. Application of a reducing potential then caused the cleavage of molecule 2, making the surface amenable to cell adhesion.

In this case, the surface chemistry developed was the modification of Si(100)–H via hydrosilylation of 1-alkynes,^{12a,d,19} which can provide good control over both surface chemistry and substrate topography.⁵ Functional monolayers on nonoxidized Si substrates are extremely robust^{12a,b} and hold considerable promise in disciplines as diverse as cell biology,^{5,20} sensing,²¹ electrochemistry,^{14a,22} molecular electronics,²³ bioelectronics,²⁴ and solar energy conversion.²⁵ In addition to being robust, the surface chemistry is modular: the same “building blocks” can be coupled to many types of surfaces, such as indium tin oxide if transparent substrates are needed, or gold if plasmonic devices are being used.

Modularity of surface chemistry has gained in importance with the increasing complexity of functional interfaces fabricated on solid surfaces. To facilitate the fabrication of complex biointerfaces in a modular fashion requires the use of building blocks with coupling schemes that are orthogonal to each other. As a consequence we, as well as others, have developed silicon modification methods^{12d,14b,20,21c,26} that employ carbodiimide²⁷ and Cu^I-catalyzed alkyne–azide cycloaddition (CuAAC) “click” reactions.²⁸ These synthetic schemes have opened entirely new, efficient, and selective routes to surface derivatization.^{12d}

Assembly of the acetylenylated Si(100) surface SAM-1 followed a previously reported procedure.^{14,29} The high quality of these surfaces was supported by X-ray photoelectron spectroscopy (XPS) and X-ray reflectometry (XRR) data (Figures 2a and 3 and Table S1).³⁰ On hydrogenated silicon surfaces, monolayer assembly with 1-alkynes yields alkenyl monolayers with a Si–C=C linkage.^{19a,b,31} In contrast to the case of Si–C–C, the Si–C=C³² linkage is known to inhibit oxidation of the underlying silicon and therefore can enhance the monolayer stability.^{12a} Click attachment of the redox-sensitive linker 2 onto SAM-1 was high yielding, with an XPS-estimated³³ extent of conversion of SAM-1 to SAM-2 close to 55%, a value consistent with other derivatizations of the base layer with similar molecules.^{14b,21c,34} The reaction of SAM-1 with azide 2 resulted in a significant decrease in the sessile water contact angle value from $82 \pm 3^\circ$ to $69 \pm 5^\circ$ for SAM-2. Increased surface hydrophilicity is consistent with the coupling of the coumarin moiety onto the acetylene surface and is in excellent agreement with values observed for other hydroquinone derivatives on Si(111).³⁵ XPS narrow-scan C 1s signals (Figure 2b) supported the formation of SAM-2 and were deconvoluted with fitting to four functions: (a) a predominant peak centered at 285 eV ascribed to aliphatic and aromatic C-bonded carbon (C–C);³⁶ (b) a signal at 286.3 eV corresponding to N-, O-, and carbonyl-bonded carbon [C–N,^{14b,37} C–O,^{31d,38} and C(O)C³⁹]; (c) a high-binding-energy signal at 289.3 eV assigned to the electron-deficient C atom in the lactone carbonyl group (O–C=O);⁴⁰ and (d) a lower-

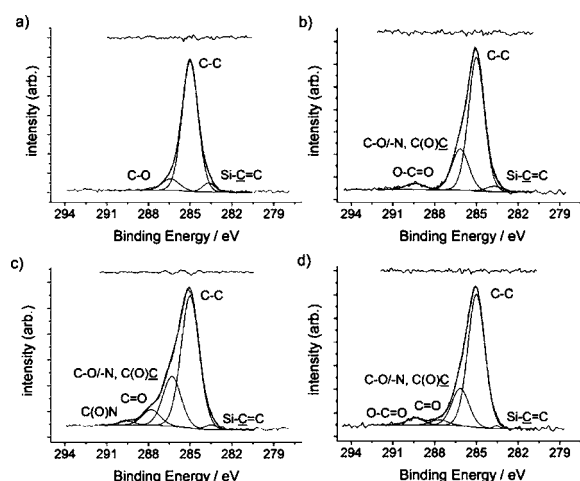


Figure 2. Attachment and further functionalization of redox-sensitive linker 2 onto Si(100) electrodes. High-resolution C 1s XPS spectrographs for (a) acetylene-terminated SAM-1, (b) dormant 2 in SAM-2, (c) OEO-decorated SAM-3, and (d) “switched” electrodes (SAM-2). The residuals of the fits are shown above the spectra.

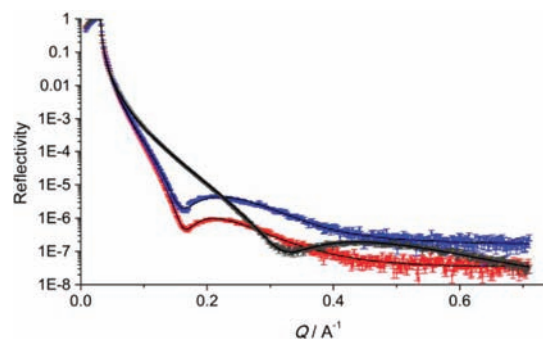


Figure 3. XRR profiles from the acetylene- (SAM-1, black curve) and OEO-functionalized (SAM-3, red curve) films. Electrochemical release of the distal OEO module is accompanied by a sizable decrease in interfacial roughness and electron density (SAM-2, blue curve). The refinement of a structural model is shown as the solid line.

binding-energy component at 283.6 eV assigned to a silylated olefin (Si–C=C).^{31d,41} Further, from the comparison of XPS and stoichiometric O–C=O:N and O–C=O:(C–O/–N/C(O)C)⁴² atomic ratios (1.2:3 and 0.9:6, respectively) it was possible to infer that the molecular nature of 2 was not altered upon its immobilization. Most importantly, XPS Si 2p narrow scans of the functionalized surface showed exceedingly minor oxidation of the substrate during the aqueous click step [SiO_x ≤ 0.06 ML equivalents; Figure S1].^{43,44}

To provide further detail on the formation of this structurally well-defined organic molecular surface, XRR measurements were performed on SAM-2. Experimental reflectivity data were fitted to a single-layer structural model (Figure S2) with the refined structural parameters summarized in Table S1. The appearance of the interference minimum at a lower value of *Q* for the SAM-2 sample indicates that its film is thicker than the 9.6 Å film of the SAM-1 monolayer. The refined thickness was 22.2(3) Å, in good agreement with the computed value.⁴⁵

To test the viability of the switchable system in cell studies and underline the modularity of the chemical approach of Figure 1, we decorated the Si(100) electrode with the OEO antifouling molecule 3.⁴⁶ Chemical oxidation of the confined lactone moiety in SAM-2 to the corresponding benzoquinone

acid was followed by its activation with carbodiimides and *N*-hydroxysuccinimide (NHS) to promote reactions of the exposed acid function toward nucleophiles (see sections S1.3 and S2 in the SI). The overall yields for SAM-3 preparation over four steps from the acetylenyl precursor (SAM-1) were close to 20% (XPS data; Figure 2c), and the high quality of the interface was demonstrated by the negligible silicon oxide-related emissions at 101–103 eV in the XPS spectra (Figure S1). The experimental C=O:C(O)N ratio (Figure 2c) was $(3.8 \pm 0.2):1$, a value larger than the ideal stoichiometric value of 2:1 for the surface product. Nonquantitative conversion for both the activation and nucleophilic displacement steps may account for this spectral feature.³⁴ The large decrease in the sessile contact angle value from $\sim 69^\circ$ for SAM-2 to $51 \pm 5^\circ$ for SAM-3 is consistent with the rendering of the surface hydrophilic upon coupling of OEO 3.^{14b,47} The presence of 3 imparted resistance to cell adhesions: only a few bovine aortic endothelial cells (BAECs) adhered to the substrate SAM-3 (Figure 4) with a rounded morphology (as distinct from well-

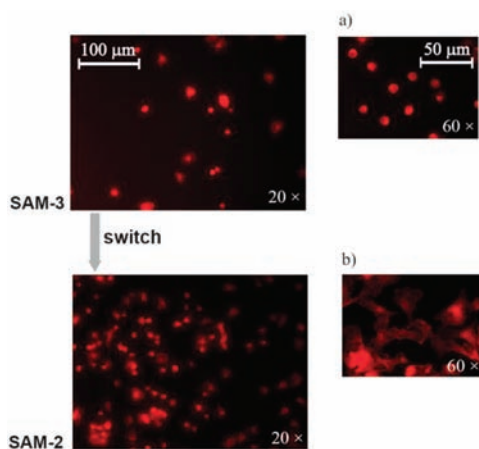


Figure 4. Fluorescence micrographs of BAECs cultured on Si SAMs presenting either OEO chains (SAM-3) or on-switched and cell-fouling substrates (SAM-2) after electrochemical removal of the protein-repellent film. Micrographs (a) and (b) show the morphological differences between adherent and nonadherent cells.

adhering cells, which spread). Reductive release of the OEO portion of the film was intended as a simplified model of a modular dynamic substrate, leading to adhesive interactions between cells and a chemically well-defined interface. The expected switch in the properties of the Si(100)-based interface were probed by cell-adhesion experiments and contact angle, XPS (Figure 2), and XRR (Figure 3) measurements. A reducing potential was applied to the working silicon electrode (-1800 mV vs Ag|AgCl|3 M NaCl) for a specified time (~ 100 s) to trigger the “trimethyl lock” and promote the intramolecular lactonization of the coumarin portion of the film. Notably, it has been shown that similar cells (bovine capillary cells) are unaffected by a potential of -1800 mV.⁴⁸

The subsequent release of the antifouling OEO portion in SAM-3 (see Figure 1) was supported by contact angle measurements, with the sessile water contact angle value increasing from $\sim 51^\circ$ prior to the switch to $65 \pm 5^\circ$, in good agreement with successful regeneration of the putative cell-fouling SAM-2. X-ray scattering length densities (SLDs)⁴⁹ and film–air roughnesses (σ_{film}) were obtained from refined XRR data⁵⁰ and are shown in Figure 3 and summarized in Table S1.

The substantial decrease in the σ_{film} and SLD values (from a poorly packed OEO layer with $\sigma_{\text{film}} = 10.2$ Å to a smoother ring-closed system with $\sigma_{\text{film}} = 6.2$ Å) is in agreement with the conversion of SAM-3 to the switched product, validating the electrochemical reduction of SAM-3 to its precursor, SAM-2.

While adhesion was greatly inhibited on OEO-functionalized surfaces,⁵¹ switching to SAM-2 was expected to provide a surface promoting cell adhesion.⁵² Endothelial cells were simultaneously plated on several (minimum six each) surface samples presenting either OEO chains (SAM-3) or lactone moieties 2 (switched samples, SAM-2). Representative fluorescence microscopy images of the fixed endothelial cells stained for F-actin are shown in Figure 4. Cells with rounded morphology having radius smaller than ~ 25 μm (Figure 4a) were considered nonadherent and were not counted.⁵³ All cells that spread and had actin stress fibers (Figure 4b) were considered adherent and were counted.^{5b} The fluorescence micrographs showed that the OEO tethered on the benzoquinone linker efficiently limited cell adhesion on those substrates. The number of adherent cells was 109 ± 21 mm⁻². Upon electrochemical cleavage of the antifouling layer, the number of adhesive cells on the surface was significantly higher (480 ± 58 mm⁻²), thus showing distinct changes in cell-adhesion properties as the surface was switched.

We have demonstrated a modular strategy for forming a structurally and chemically well-defined substrate where surface properties relevant to tissue culturing can be dynamically switched. The chemical modules and assembly protocols described here were performed on silicon surfaces because of the highly stable surface chemistry,^{12d} the compatibility of this material with the microelectronics industry,¹⁰ the ease of microfabrication and nanostructuring of the substrate,^{5b,54} and the tunable electrical⁵⁵ and optical properties of silicon.^{21b} However, the same surface chemistry could equally well be used on any alkyne-terminated surface and thus could be applied in various fields such as cell-based sensors and electrochemical devices. This new surface chemistry can contribute to the emerging field of artificial substrates for cell biology and is an important step toward the controlled temporal manipulation of cells and their environments.

■ ASSOCIATED CONTENT

📄 Supporting Information

Experimental section and XPS and XRR data. This material is available free of charge via the Internet at <http://pubs.acs.org>.

■ AUTHOR INFORMATION

✉ Corresponding Author

justin.gooding@unsw.edu.au

■ ACKNOWLEDGMENTS

This research was supported by the Australian Research Council’s Discovery Projects Funding Scheme (DP1094564). S.C. was supported by an International Postgraduate Research Scholarship from the Australian Government and by a Research Postgraduate Award from the Australian Institute of Nuclear Science and Engineering (AINSE).

■ REFERENCES

- (1) Gumbiner, B. M. *Cell* **1996**, *84*, 345.
- (2) Geiger, B.; Spatz, J. P.; Bershadsky, A. D. *Nat. Rev. Mol. Cell Biol.* **2009**, *10*, 21.
- (3) Mrksich, M. *Chem. Soc. Rev.* **2000**, *29*, 267.

- (4) Pulsipher, A.; Yousaf, M. N. *ChemBioChem* **2010**, *11*, 745.
- (5) (a) Le Saux, G.; Magenau, A.; Gunaratnam, K.; Kilian, K. A.; Böcking, T.; Gooding, J. J.; Gaus, K. *Biophys. J.* **2011**, *101*, 764. (b) Le Saux, G.; Magenau, A.; Böcking, T.; Gaus, K.; Gooding, J. J. *PLoS One* **2011**, *6*, No. e21869.
- (6) (a) Yousaf, M. N. *Curr. Opin. Chem. Biol.* **2009**, *13*, 697. (b) Robertus, J.; Browne, W. R.; Feringa, B. L. *Chem. Soc. Rev.* **2010**, *39*, 354. (c) Mrksich, M. *Curr. Opin. Chem. Biol.* **2002**, *6*, 794.
- (7) (a) Yeo, W.-S.; Hodneland, C. D.; Mrksich, M. *ChemBioChem* **2001**, *2*, 590. (b) Yousaf, M. N.; Houseman, B. T.; Mrksich, M. *Angew. Chem., Int. Ed.* **2001**, *40*, 1093.
- (8) Lamb, B. M.; Yousaf, M. N. *J. Am. Chem. Soc.* **2011**, *133*, 8870.
- (9) Buriak, J. M. *Chem. Rev.* **2002**, *102*, 1271.
- (10) Ball, P. *Nat. Mater.* **2005**, *4*, 119.
- (11) (a) Bent, S. F.; Kachian, J. S.; Rodríguez-Reyes, J. C. F.; Teplyakov, A. V. *Proc. Natl. Acad. Sci. U.S.A.* **2011**, *108*, 956. (b) Rijksen, B.; van Lagen, B.; Zuilhof, H. J. *Am. Chem. Soc.* **2011**, *133*, 4998.
- (12) (a) Puniredd, S. R.; Assad, O.; Haick, H. *J. Am. Chem. Soc.* **2008**, *130*, 13727. (b) Sieval, A. B.; Demirel, A. L.; Nissink, J. W. M.; Linford, M. R.; van der Maas, J. H.; de Jeu, W. H.; Zuilhof, H.; Sudhölter, E. J. R. *Langmuir* **1998**, *14*, 1759. (c) Sieval, A. B.; Linke, R.; Zuilhof, H.; Sudhölter, E. J. R. *Adv. Mater.* **2000**, *12*, 1457. (d) Ciampi, S.; Harper, J. B.; Gooding, J. J. *Chem. Soc. Rev.* **2010**, *39*, 2158.
- (13) Kandere-Grzybowska, K.; Campbell, C.; Komarova, Y.; Grzybowski, B. A.; Borisy, G. G. *Nat. Methods* **2005**, *2*, 739.
- (14) (a) Ciampi, S.; Eggers, P. K.; Le Saux, G.; James, M.; Harper, J. B.; Gooding, J. J. *Langmuir* **2009**, *25*, 2530. (b) Ciampi, S.; Böcking, T.; Kilian, K. A.; James, M.; Harper, J. B.; Gooding, J. J. *Langmuir* **2007**, *23*, 9320.
- (15) Synthetic procedures for the preparation of the redox-sensitive lactone linker **2** in 10 steps from commercially available 2,5-dimethylphenol are given in the SI.
- (16) Milstien, S.; Cohen, L. A. *Proc. Nat. Acad. Sci. U.S.A.* **1970**, *67*, 1143.
- (17) Borchardt, R. T.; Cohen, L. A. *J. Am. Chem. Soc.* **1972**, *94*, 9166.
- (18) Zheng, A.; Shan, D.; Wang, B. *J. Org. Chem.* **1999**, *64*, 156.
- (19) (a) Linford, M. R.; Fenter, P.; Eisenberger, P. M.; Chidsey, C. E. D. *J. Am. Chem. Soc.* **1995**, *117*, 3145. (b) Scheres, L.; Giesbers, M.; Zuilhof, H. *Langmuir* **2010**, *26*, 10924. (c) Ng, A.; Ciampi, S.; James, M.; Harper, J. B.; Gooding, J. J. *Langmuir* **2009**, *25*, 13934.
- (20) Li, Y.; Santos, C. M.; Kumar, A.; Zhao, M.; Lopez, A. I.; Qin, G.; McDermott, A. M.; Cai, C. *Chem.—Eur. J.* **2011**, *17*, 2656.
- (21) (a) Hamers, R. J. In *Bioelectronics: From Theory to Applications*; Willner, I., Katz, E., Eds.; Wiley-VCH: Weinheim, Germany, 2005; p 209. (b) Guan, B.; Magenau, A.; Kilian, K. A.; Ciampi, S.; Gaus, K.; Reece, P. J.; Gooding, J. J. *Faraday Discuss.* **2011**, *149*, 301. (c) Ciampi, S.; James, M.; Michaels, P.; Gooding, J. J. *Langmuir* **2011**, *27*, 6940.
- (22) Fabre, B. *Acc. Chem. Res.* **2010**, *43*, 1509.
- (23) Vilan, A.; Yaffe, O.; Biller, A.; Salomon, A.; Kahn, A.; Cahen, D. *Adv. Mater.* **2010**, *22*, 140.
- (24) Ciampi, S.; Gooding, J. J. *Chem.—Eur. J.* **2010**, *16*, 5961.
- (25) Har-Lavan, R.; Ron, I.; Thieblemont, F.; Cahen, D. *Appl. Phys. Lett.* **2009**, *94*, No. 043308.
- (26) Qin, G.; Santos, C.; Zhang, W.; Li, Y.; Kumar, A.; Erasquin, U. J.; Liu, K.; Muradov, P.; Trautner, B. W.; Cai, C. *J. Am. Chem. Soc.* **2010**, *132*, 16432.
- (27) Voicu, R.; Boukherroub, R.; Bartzoka, V.; Ward, T.; Wojtyk, J. T. C.; Wayner, D. D. M. *Langmuir* **2004**, *20*, 11713.
- (28) (a) Tornøe, C. W.; Christensen, C.; Meldal, M. *J. Org. Chem.* **2002**, *67*, 3057. (b) Rostovtsev, V. V.; Green, L. G.; Fokin, V. V.; Sharpless, K. B. *Angew. Chem., Int. Ed.* **2002**, *41*, 2596.
- (29) (a) James, M.; Darwish, T. A.; Ciampi, S.; Sylvester, S. O.; Zhang, Z.; Ng, A.; Gooding, J. J.; Hanley, T. L. *Soft Matter* **2011**, *7*, 5309. (b) James, M.; Ciampi, S.; Darwish, T. A.; Hanley, T. L.; Sylvester, S. O.; Gooding, J. J. *Langmuir* **2011**, *27*, 10753. (c) Ciampi, S.; James, M.; Darwish, N.; Luais, E.; Guan, B.; Harper, J. B.; Gooding, J. J. *Phys. Chem. Chem. Phys.* **2011**, *13*, 15624.
- (30) The structure of the adventitious C–O bond has not been fully elucidated, although the contamination has been reported in several works (see refs 21c, 31a, 31d, and 38).
- (31) (a) Kondo, M.; Mates, T. E.; Fischer, D. A.; Wudl, F.; Kramer, E. J. *Langmuir* **2010**, *26*, 17000. (b) Cicero, R. L.; Linford, M. R.; Chidsey, C. E. D. *Langmuir* **2000**, *16*, 5688. (c) Scheres, L.; Giesbers, M.; Zuilhof, H. *Langmuir* **2010**, *26*, 4790. (d) Scheres, L.; Arafat, A.; Zuilhof, H. *Langmuir* **2007**, *23*, 8343.
- (32) The double bond near the surface also increases the coupling between the organic monolayer and the silicon, increasing the contact conductance (see ref 41).
- (33) Combined quantitative N 1s and C 1s XPS data (C–C:N).
- (34) Gooding, J. J.; Ciampi, S. *Chem. Soc. Rev.* **2011**, *40*, 2704.
- (35) Rohde, R. D.; Agnew, H. D.; Yeo, W.-S.; Bailey, R. C.; Heath, J. R. *J. Am. Chem. Soc.* **2006**, *128*, 9518.
- (36) Lehner, A.; Steinhoff, G.; Brandt, M. S.; Eickhoff, M.; Stutzmann, M. *J. Appl. Phys.* **2003**, *94*, 2289.
- (37) (a) Baio, J. E.; Weidner, T.; Brison, J.; Graham, D. J.; Gamble, L. J.; Castner, D. G. *J. Electron Spectrosc. Relat. Phenom.* **2009**, *172*, 2. (b) Böcking, T.; James, M.; Coster, H. G. L.; Chilcott, T. C.; Barrow, K. D. *Langmuir* **2004**, *20*, 9227.
- (38) Wallart, X.; de Villeneuve, C. H.; Allongue, P. *J. Am. Chem. Soc.* **2005**, *127*, 7871.
- (39) Zhong, Y. L.; Bernasek, S. L. *J. Am. Chem. Soc.* **2011**, *133*, 8118.
- (40) Briggs, D.; Seah, M. P. *Practical Surface Analysis by Auger and X-ray Photoelectron Spectroscopy*; Wiley: Chichester, U.K., 1983.
- (41) Yaffe, O.; Scheres, L.; Segev, L.; Biller, A.; Ron, I.; Salomon, E.; Giesbers, M.; Kahn, A.; Kronik, L.; Zuilhof, H.; Vilan, A.; Cahen, D. *J. Phys. Chem. C* **2010**, *114*, 10270.
- (42) Sum of photoemissions for N-, O-, and carbonyl-bonded carbons [C–N, C–O, and C(O)C, respectively].
- (43) When the fractional monolayer was present, the coverage of oxidized silicon was calculated directly from the oxidized/bulk Si 2p peak-area ratio using the method described by Lewis and co-workers (ref 44). SiO_x levels for SAM-2 were either below or very close to the spectrometer detection limit (ca. 0.06 SiO_x ML equivalents).
- (44) (a) Webb, L. J.; Lewis, N. S. *J. Phys. Chem. B* **2003**, *107*, 5404. (b) Haber, J. A.; Lewis, N. S. *J. Phys. Chem. B* **2002**, *106*, 3639.
- (45) From the analysis of energy-minimized structures (semi-empirical MOPAC calculations, Chem3D Ultra), the distance separating Si atop atoms and the C(O)O of the coumarin moiety was 22.1 Å for SAM-2.
- (46) See the SI for the experimental protocols for the oxidation of the confined lactone molecule to the corresponding benzoquinone acid followed by its activation with carbodiimides and N-hydroxysuccinimide to promote reactions of the exposed acid function toward nucleophiles.
- (47) (a) Böcking, T.; Gal, M.; Gaus, K.; Gooding, J. J. *Aust. J. Chem.* **2005**, *58*, 660. (b) Yam, C. M.; Lopez-Romero, J. M.; Gu, J.; Cai, C. *Chem. Commun.* **2004**, 2510.
- (48) Jiang, X.; Ferrigno, R.; Mrksich, M.; Whitesides, G. M. *J. Am. Chem. Soc.* **2003**, *125*, 2366.
- (49) For X-rays, electron densities (e Å⁻³) of the film were obtained by dividing the SLD values by the factor 2.82 × 10⁻⁵ Å.
- (50) Nelson, A. J. *Appl. Crystallogr.* **2006**, *39*, 273.
- (51) Roberts, C.; Chen, C. S.; Mrksich, M.; Martichonok, V.; Ingber, D. E.; Whitesides, G. M. *J. Am. Chem. Soc.* **1998**, *120*, 6548.
- (52) Sethuraman, A.; Han, M.; Kane, R. S.; Belfort, G. *Langmuir* **2004**, *20*, 7779.
- (53) Endothelial cells, provided that suitable amounts of nutrients are supplied, survive only when they are able to adhere and spread, whereas a large fraction of nonadherent (rounded) cells enter apoptosis. Earlier works by Whiteside and Mrksich explored many of the factors affecting endothelial cell shape and how this relates to whether individual cells grow or die. See: Chen, C. S.; Mrksich, M.; Huang, S.; Whitesides, G. M.; Ingber, D. E. *Science* **1997**, *276*, 1425.
- (54) Sailor, M. J.; Link, J. R. *Chem. Commun.* **2005**, 1375.
- (55) Zigah, D.; Herrier, C.; Scheres, L.; Giesbers, M.; Fabre, B.; Hapiot, P.; Zuilhof, H. *Angew. Chem., Int. Ed.* **2010**, *49*, 3157.